

Stem Cell Reports, Volume 9

Supplemental Information

A COUP-TFII Human Embryonic Stem Cell Reporter Line to Identify and Select Atrial Cardiomyocytes

Verena Schwach, Arie O. Verkerk, Mervyn Mol, Jantine J. Monshouwer-Kloots, Harsha D. Devalla, Valeria V. Orlova, Konstantinos Anastassiadis, Christine L. Mummery, Richard P. Davis, and Robert Passier

Supplemental material

- Figures S1-7
- Table S1-3
- Supplemental Experimental Methods
- Supplemental videos 1-4
- Supplemental references

Supplemental Figures

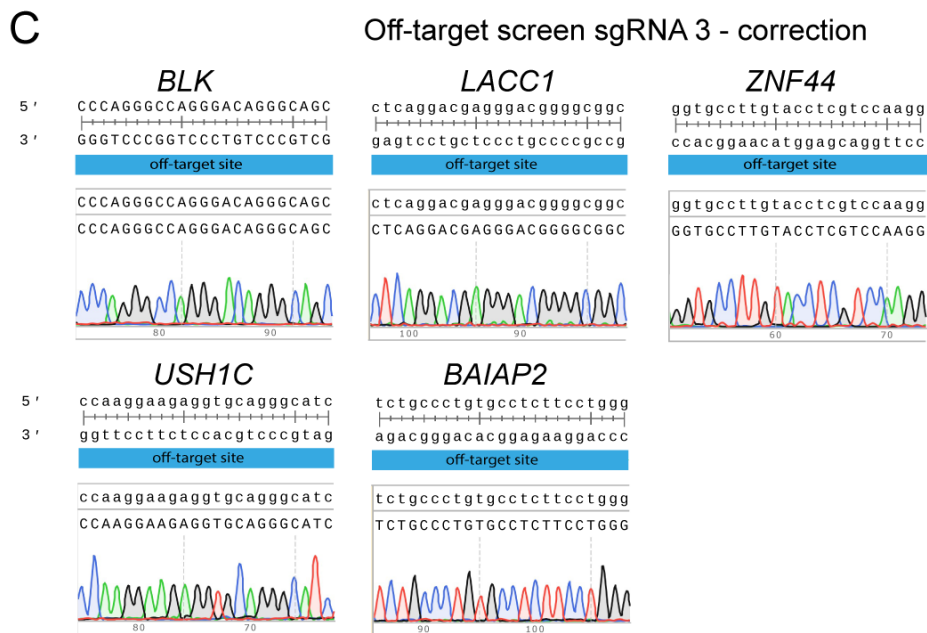
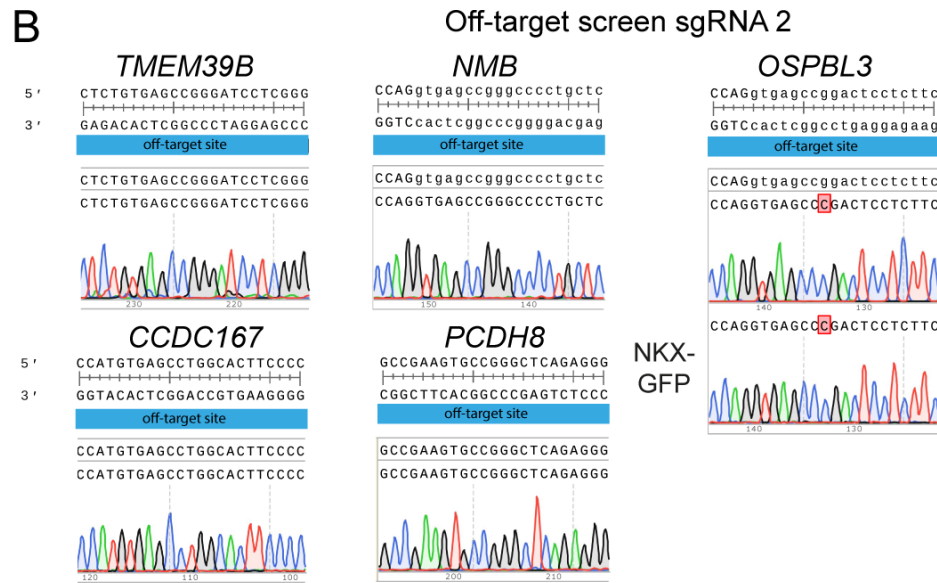
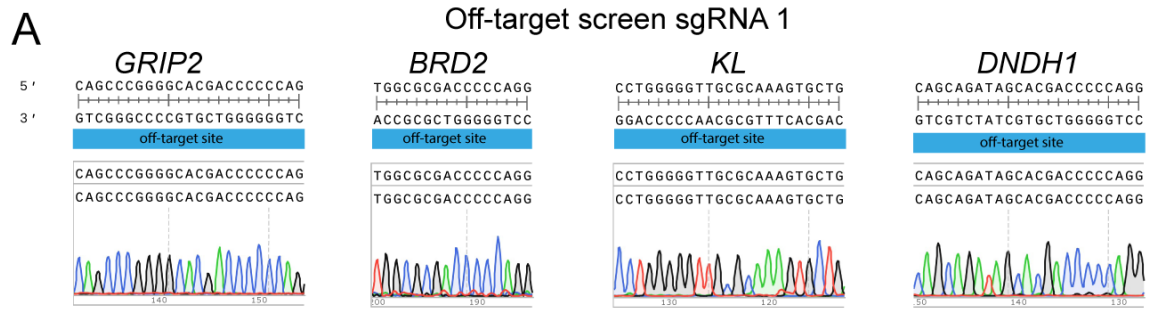
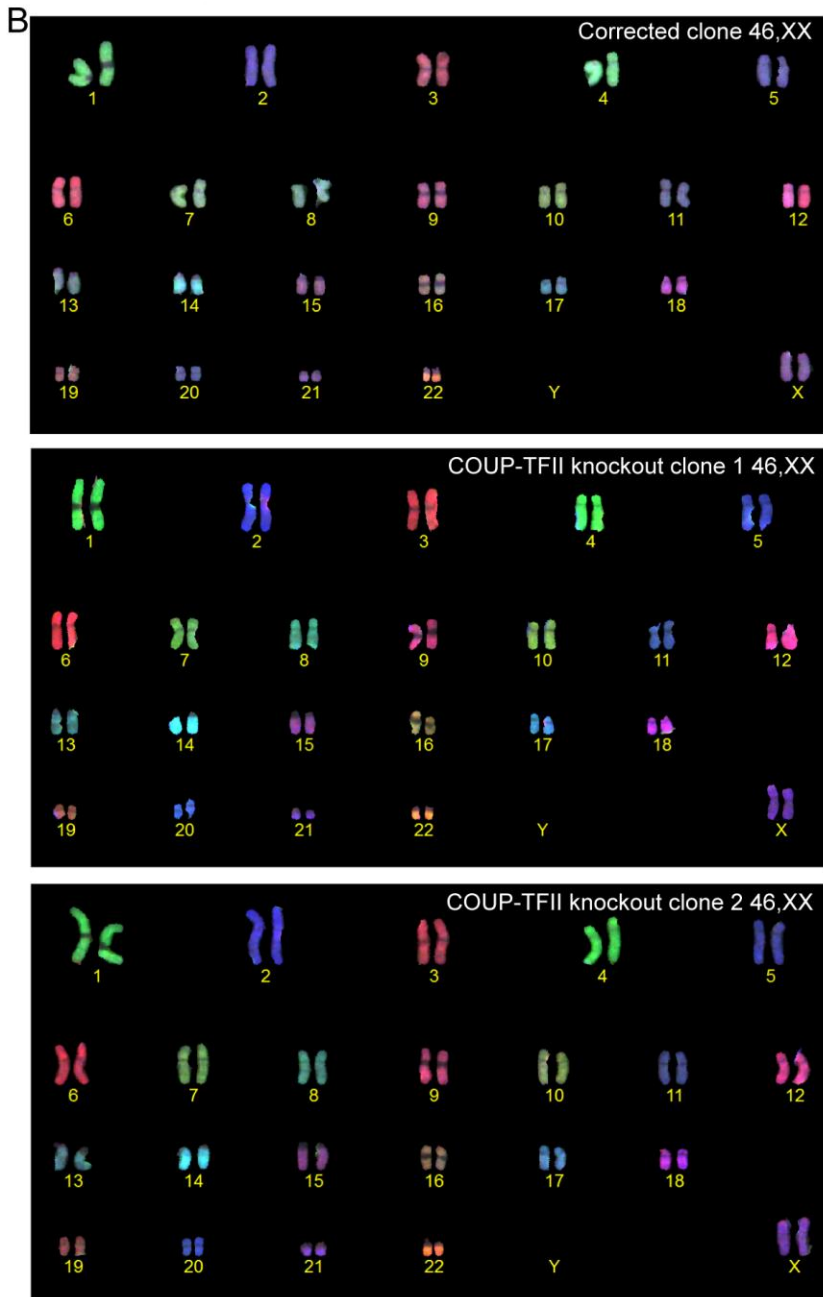
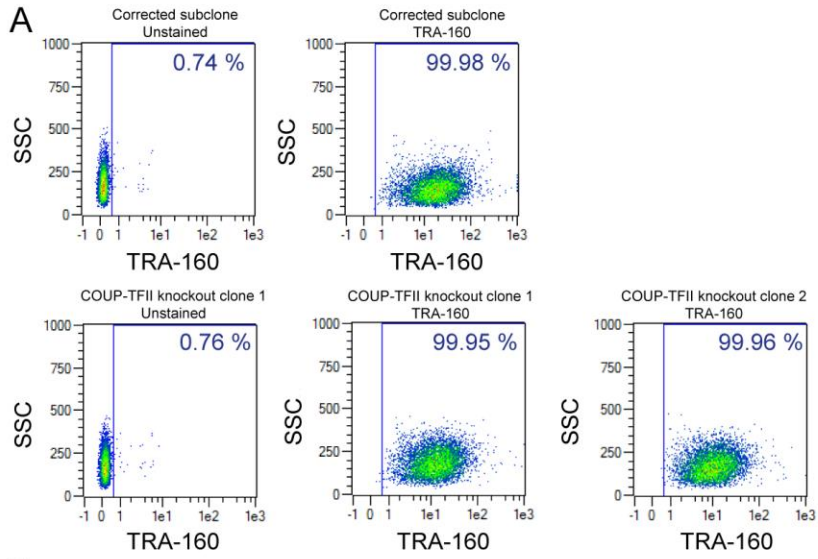


Figure S1: Off-target screen following CRISPR/Cas9-mediated genome editing. Related to Figure 1. A) Top-candidates of predicted off-target sites of sgRNA 1 with 3 mismatches (GRIP2 and KL), 4 mismatches (DNDH1) or shorter sequence overlap (BRD2). B) Off-targets of sgRNA 2 with at least four mismatches. For sgRNA 2, a polymorphism in OSPBL3 was already present in the parental NKX-GFP line. C) Off-targets of sgRNA 3 with three mismatches.



**Figure S2: A) Flow cytometry for the stem cell marker TRA-1-6-0 and B) karyotyping.
Related to Figure 1.**

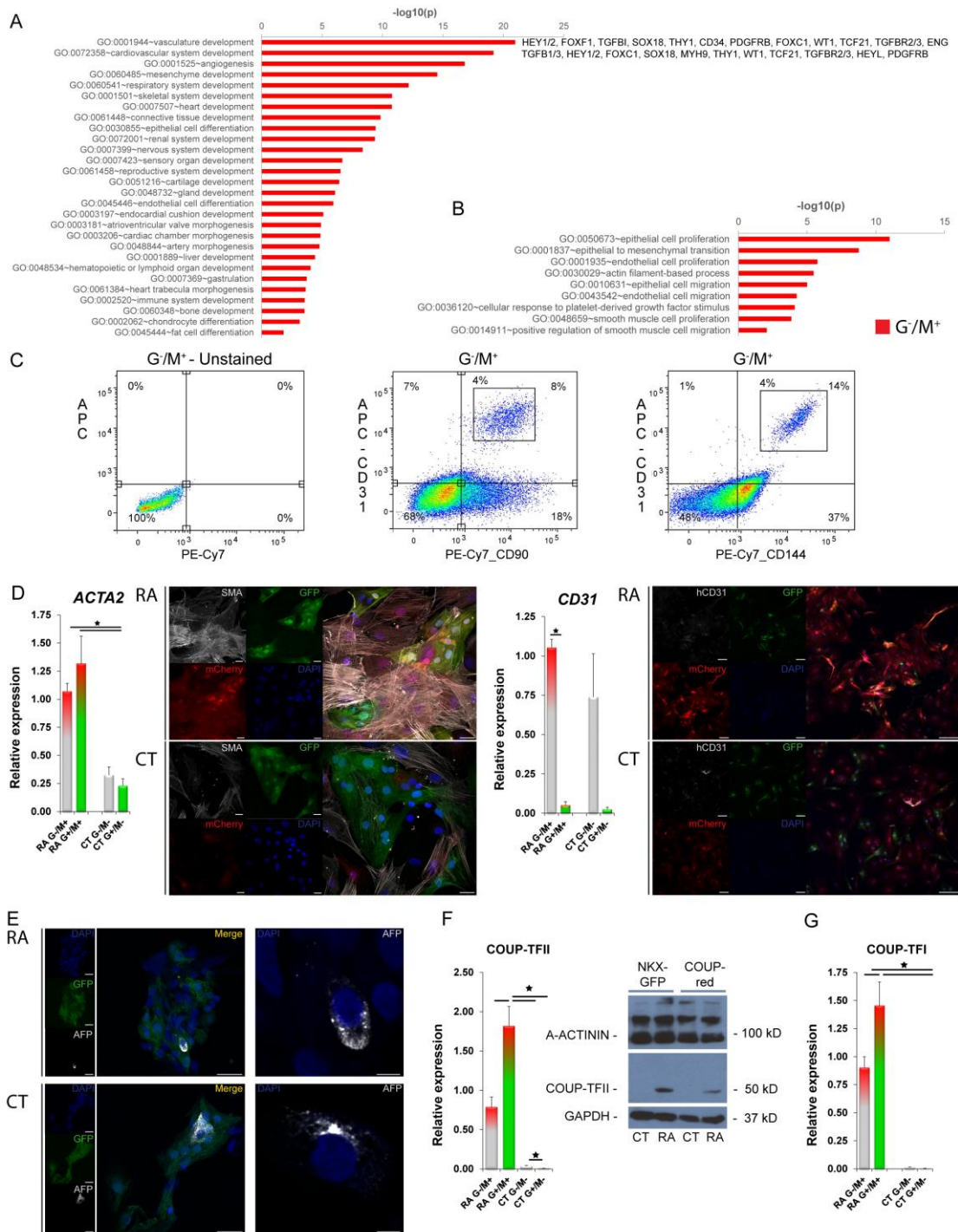


Figure S3: Identity of mCherry-positive non-CMs. Related to Figure 2 and 3. A and B) Gene ontology (GO) enrichment analysis of upregulated transcripts in GFP(G)-/mCherry(M)+ cells compared to G+/M+ CMs. C) Flow cytometry of CD90 (Thy-1) CD31 (PECAM) and CD144 (VE-Cadherin) in G-/M+ cells at day 13 of differentiation. D) Smooth muscle actin (*ACTA2*) and CD31 mRNA quantified in sorted G/M populations ($n=3$; mean \pm SEM). Protein expression of smooth muscle actin (SMA) (Scale bar = 25 μ m) and CD31 (Scale bar = 100 μ m) in unsorted dissociated cells from RA-treated and CT condition in combination with fluorescently labeled mCherry, DAPI and endogenous expression of GFP at day 20 of differentiation. E) α -fetoprotein (AFP) immunostaining of unsorted dissociated cells from RA-treated and CT conditions in combination with DAPI and endogenous expression of GFP. Scale

bar = 25 μm (left) and 5 μm (right). F) mRNA expression of COUP-TFII in sorted G/M populations from RA and CT differentiations at day 20 of differentiation (n=3; mean \pm SEM) and Western blot of COUP-TFII in unsorted samples of differentiated CMs from RA and CT differentiations from COUP-red compared to NKX-GFP cells at day 20 of differentiation. G) mRNA expression of COUP-TFI in sorted G/M populations from RA and CT condition at day 20 of differentiation (n=3; mean \pm SEM).

of one Cytosine (C) residue within exon 1 in one allele of COUP-TFII, whereas the other allele was targeted with mCherry. D) Premature stopcodon introduced by sgRNA 2 marked with an asterix. E) Schematic overview of WT COUP-TFII, COUP-TFII-mCherry knock-in allele, and COUP-TFII knockout allele.

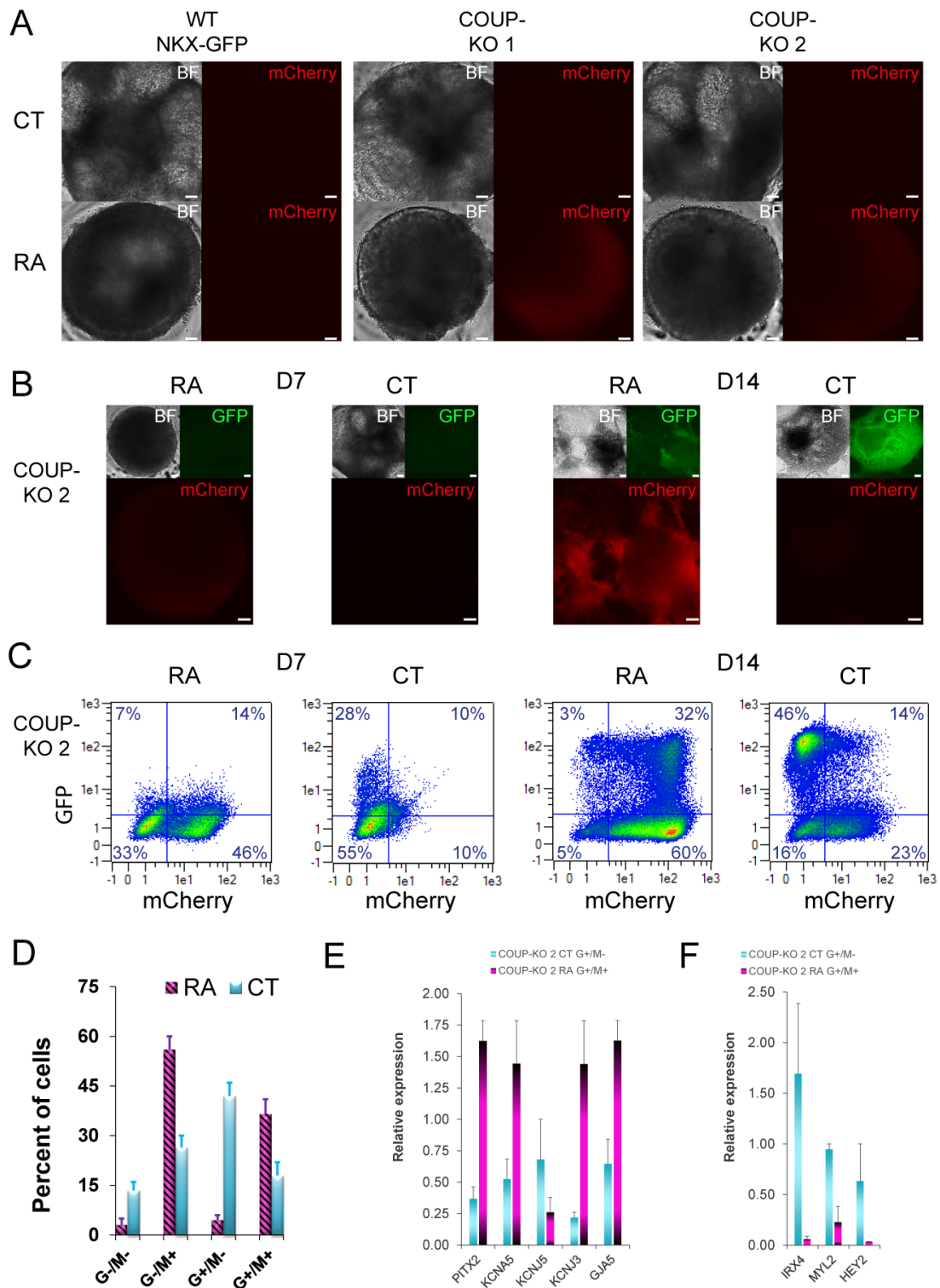


Figure S5: Characterization of COUP-KO lines. Related to Figure 4 and 6. A) mCherry overlapping with brightfield (BF) images at D6 of differentiation in retinoic acid (RA) or control (CT) differentiations from wildtype (WT) NKX-GFP or subclones COUP-KO 1 and 2. Scale bar = 100 μ m. B) mCherry overlapping with GFP and brightfield (BF) images at D7 and D14 of differentiation in RA or CT differentiations from WT NKX-GFP or COUP-KO 2 cells. Scale bar = 100 μ m. C) Representative FACS plots depicting the percentage of GFP/mCherry populations at D7 and D14 of differentiation in RA or CT differentiations from WT NKX-GFP or COUP-KO 2. D) Averaged GFP/mCherry percentage calculated from two independent differentiations at day 14 of differentiation (n=2; mean \pm SEM). E) Quantitative PCR analysis

of selected atrial-specific transcripts in sorted COUP-KO 2-derived G+/M+ fractions from RA and G+/M- populations from CT at D14 (n=2). F) Quantitative PCR analysis of selected ventricular-specific transcripts of sorted COUP-KO 2 derived G+/M+ fractions from RA and G+/M- populations from CT at D14 (n=2).

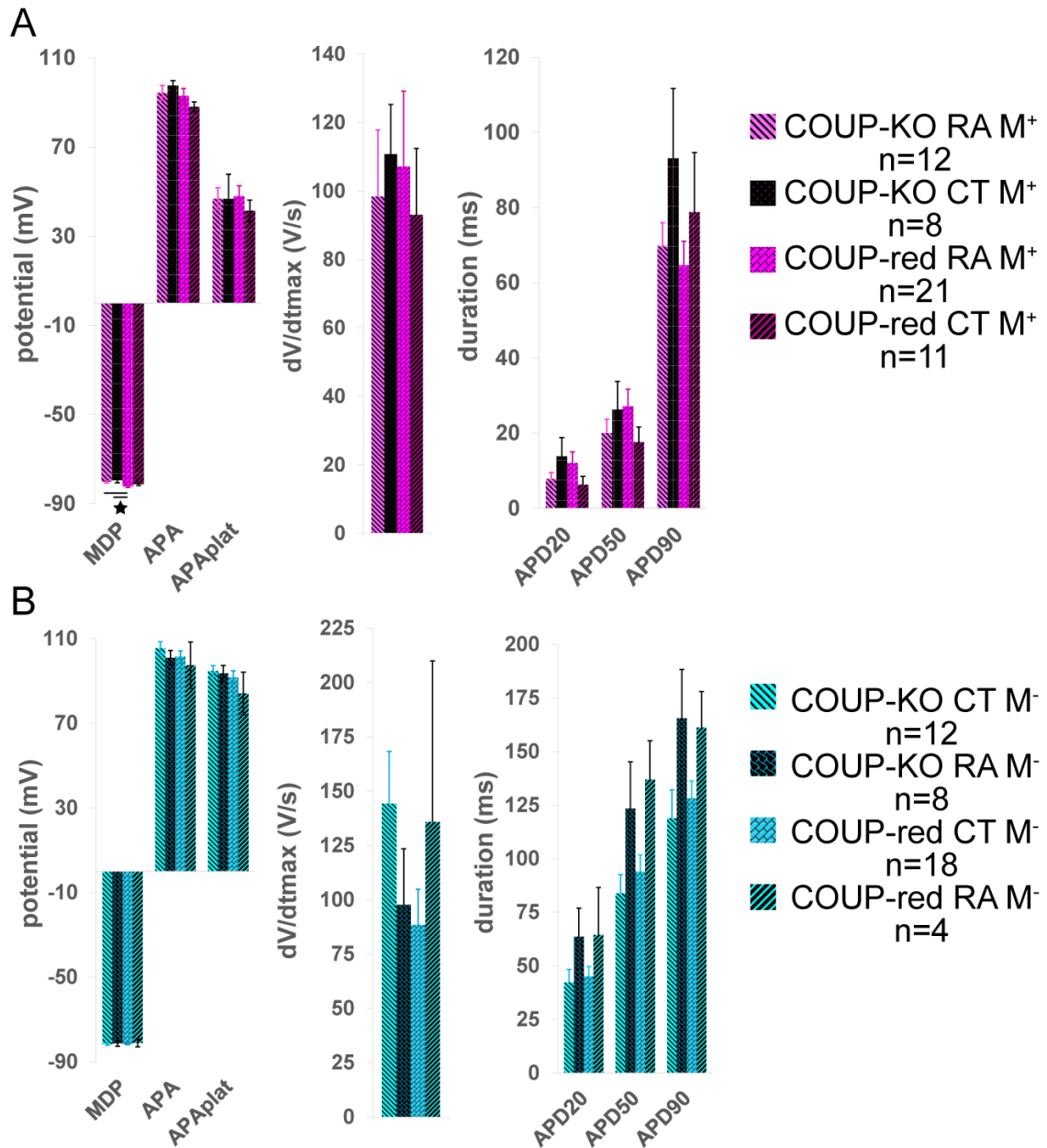


Figure S6: Electrophysiological characterization of G⁺/M⁺ CMs from CT and G⁺/M⁻ CMs from RA condition. Related to Figure 4 and 6. A) mCherry-positive CMs have atrial action potential (AP) properties (n=12 for COUP-KO RA G⁺/M⁺, n=8 for COUP-KO CT G⁺/M⁺, n=21 for COUP-red RA G⁺/M⁺, n=11 for COUP-red CT G⁺/M⁺). B) mCherry-negative CMs have ventricular AP properties (n=12 for COUP-KO CT G⁺/M⁻, n=8 for COUP-KO RA G⁺/M⁻, n=18 for COUP-red CT G⁺/M⁻, n=4 for COUP-red RA G⁺/M⁻).

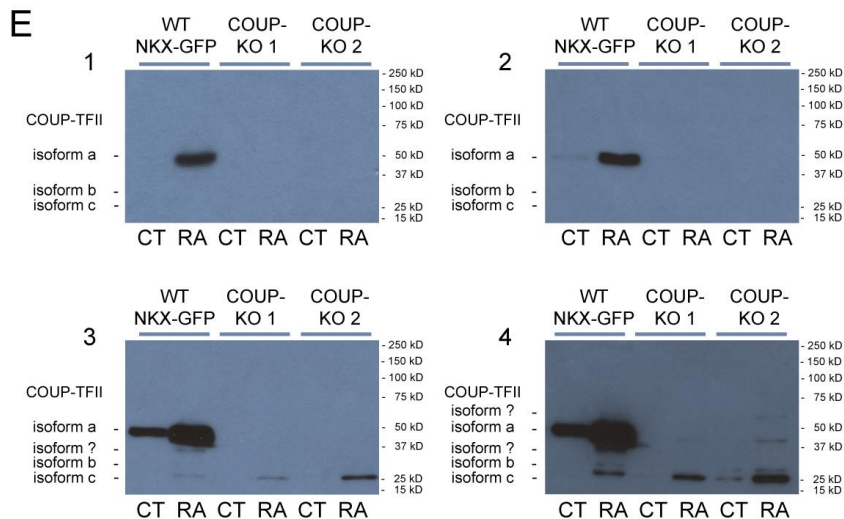
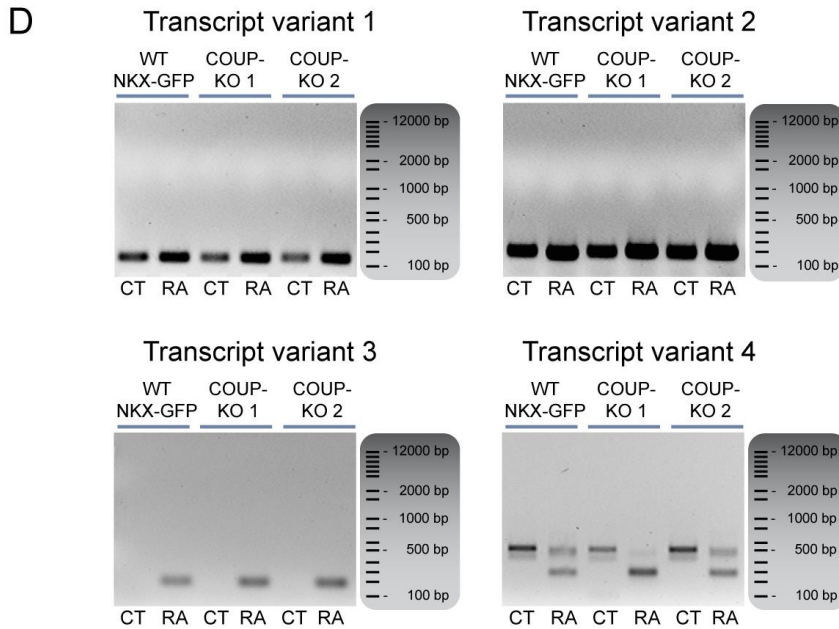
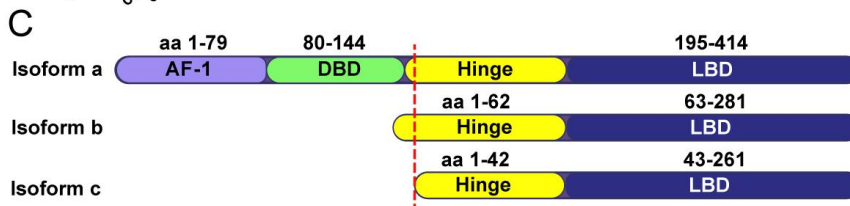
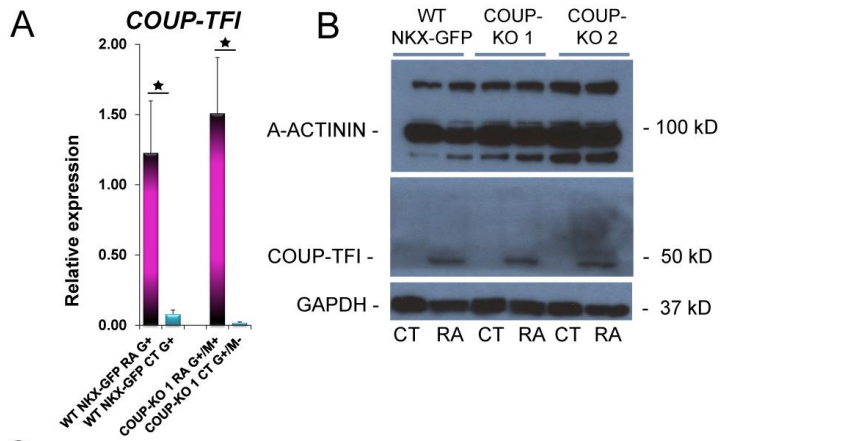


Figure S7: Expression of COUP-TFII homologue COUP-TFI and COUP-TFII isoforms. Related to Figure 4, 5, and 6. A) mRNA and B) protein expression of COUP-TFI in differentiated CMs generated from COUP-KO or WT NKX-GFP lines. C) Structural representation of protein isoforms of COUP-TFII; AF: activation function; DBD: DNA-binding domain; LBD: Ligand-binding domain. D) qPCR-end point analysis of COUP-TFII transcript variants 1-4 in sorted RA-treated M⁺ and M⁻ CMs from CT conditions of COUP-KO 1 and 2 cells in comparison to CMs from WT NKX-GFP. E) WB of COUP-TFII isoforms in unsorted RA or CT samples from COUP-KO 1 and 2 or WT NKX-GFP cells with increasing exposure time from 1 to 4.

Supplemental Tables

Table S1: Raw data of the AP characterization.

COUP-red reporter

	COUP-red CT/M ⁻ n=18	COUP-red RA/M ⁺ n=21	COUP-red CT/M ⁺ n=4	COUP-red RA/M ⁻ n=11
MDP (mV)	-81.62 ± 0.36	-82.29 ± 0.44	-81.31 ± 0.54	-81.12 ± 1.84
APA_{max} (mV)	101.49 ± 2.71	92.96 ± 3.32	87.99 ± 2.19	97.47 ± 10.94
APA_{plat} (mV)	91.62 ± 3.18	47.94 ± 4.67	41.36 ± 4.79	84.12 ± 10.08
dV/dt (V/s)	88.47 ± 16.45	107.17 ± 22.08	93.04 ± 19.41	135.83 ± 74.10
APD₂₀ (ms)	45.17 ± 4.55	12.05 ± 2.98	6.26 ± 2.23	64.43 ± 22.14
APD₅₀ (ms)	93.93 ± 7.84	27.13 ± 4.56	17.62 ± 4.03	136.91 ± 18.13
APD₉₀ (ms)	128.15 ± 8.10	64.70 ± 6.37	78.83 ± 15.84	161.22 ± 16.78

WT NKX-GFP

	NKX-GFP CT n=13	NKX-GFP RA n=12
MDP (mV)	-81.06 ± 0.43	-80.35 ± 0.71
APA_{max} (mV)	101.11 ± 2.70	99.69 ± 4.38
APA_{plat} (mV)	91.99 ± 2.45	49.28 ± 5.93
dV/dt (V/s)	141.71 ± 16.81	154.22 ± 30.83
APD₂₀ (ms)	48.55 ± 5.79	23.41 ± 7.10
APD₅₀ (ms)	91.22 ± 7.69	72.09 ± 8.25
APD₉₀ (ms)	126.94 ± 9.48	80.22 ± 8.06

COUP-KO 1

	COUP-KO 1 CT/M ⁻ n=12	COUP-KO 1 RA/M ⁺ n=12	COUP-KO 1 CT/M ⁺ n=8	COUP-KO 1 RA/M ⁻ n=8
MDP (mV)	-81.60 ± 0.63	-80.23 ± 0.49	-79.51 ± 1.10	-81.34 ± 1.30
APA_{max} (mV)	105.52 ± 3.07	94.26 ± 3.33	97.55 ± 2.24	100.94 ± 3.43
APA_{plat} (mV)	94.66 ± 2.62	46.85 ± 4.99	46.68 ± 11.08	93.57 ± 3.75
dV/dt (V/s)	144.31 ± 24.02	98.41 ± 19.50	110.79 ± 14.51	97.72 ± 25.72
APD₂₀ (ms)	42.33 ± 5.99	7.85 ± 1.70	13.83 ± 5.00	63.57 ± 13.40
APD₅₀ (ms)	83.85 ± 8.74	20.02 ± 3.64	26.27 ± 7.50	123.39 ± 21.84
APD₉₀ (ms)	118.96 ± 13.14	69.85 ± 6.11	93.16 ± 18.54	165.55 ± 22.79

COUP-KO 2

	COUP-KO 2 CT/M ⁻ n=13	COUP-KO 2 RA/M ⁺ n=14
MDP (mV)	-82.11 ± 0.63	-81.60 ± 0.63
APA_{max} (mV)	106.63 ± 2.98	101.12 ± 5.90
APA_{plat} (mV)	92.70 ± 2.42	39.15 ± 4.50
dV/dt (V/s)	174.26 ± 24.37	157.53 ± 41.57
APD₂₀ (ms)	43.20 ± 7.38	5.28 ± 0.98
APD₅₀ (ms)	96.59 ± 10.19	19.66 ± 5.51
APD₉₀ (ms)	125.29 ± 10.32	67.88 ± 8.54

Table S2: Transcript variants of human *COUP-TFII (NR2F2)*

Variant	Protein isoform	Transcript name	Ensembl ID	RefSeq	Base pairs	Biotype	Protein	Mouse orthologue
1	a	<i>NR2F2-001</i>	ENST0000000394166.7	NM_021005	5275	Protein coding	414 aa	100%
2	b	<i>NR2F2-002</i>	ENST0000000421109.6	NM_00145155	2214	Protein coding	281 aa	100%
3	c	<i>NR2F2-201</i>	ENST0000000394171.6	NM_00145156	3501	Protein coding	261 aa	-
4	c	<i>NR2F2-003</i>	ENST0000000453270.2	NM_00145157	1712	Protein coding	261 aa	-
5	-	<i>NR2F2-004</i>	ENST0000000559679.1	-	382	Protein coding	93 aa	-
6	-	<i>NR2F2-202</i>	ENST0000000410719.1	NR_031715	47	miRNA	-	-

Table S2: Transcript variants of human *COUP-TFII (NR2F2)*. Information adapted from Ensembl and NCBI (aa: amino acids).

Table S3: Microarray transcripts as separate excel file

Supplemental Experimental Procedures

Vector construction

The COUP-TFII-mCherry targeting vector (TV) was generated in 3 steps by first subcloning 15.5 kb homology sequences from a BAC carrying the human COUP-TFII (NR2F2) gene (RP11-134D15) into a p15A-amp vector via recombineering with the following oligos: hNR2F2-sub1 and hNR2F2-sub2. In the second step the mCherry-pA-FRT-PGK-BSD-pA-FRT cassette was inserted directly after the initiating Methionine (ATG) in exon 1 of NR2F2-001 transcript (ENSEMBL ID: ENST00000394166.7) using the following oligos: hNR2F2-cherry-Q1 and hNR2F2-pA-Q2. By insertion of the mCherry cassette, 57 bp downstream of the ATG were deleted to allow selection of sgRNAs that recognize only the WT but not the targeted allele. The TV had 5' homology arm (HA) of 9.6 kb and 3'HA of 5.9 kb. In the 3rd step the HAs were further shortened to 733 bp 5' and 882 bp 3' by AfeI digestion and cloning into pCR4-TOPO vector (Invitrogen) to allow PCR-mediated screening of correct targeted events. All plasmids for transfection were isolated using the Nucleobond Xtra Midi kit (Macherey-Nagel) and confirmed by sequencing (Macrogen).

hESC transfection and clonal isolation

24-48 hours after transfection, the cells were treated with 0.5 µg/ml puromycin for 48-72 hours. With transfections including the COUP-TFII-mCherry targeting vector, an additional selection with 1 µg/ml blasticidin was performed ~6 days after transfection and continued for 5-6 days. For excision of the blasticidin resistance cassette, hESCs were transfected with 1 µg of a flippase expression vector as described above and treated with 0.5 µg/ml puromycin for 48 - 72 hours starting 24 hours after transfection (Vector maps available in Supplemental Experimental Procedures). The resulting antibiotic-resistant hESCs were expanded and were either manually picked as colonies or clonally isolated by single-cell deposition using a BD ARIA III flow cytometer.

Sequences of oligos for target vector construction, sgRNAs and COUP-TFII WT ss-oligo

	(5' – 3')
hNR2F2-sub1	GTGCATTTAAGGAGATTGGGAGACAATTAGCAGAATGGAGAA AGTAAGTCATTTAAATGCGATCGCGCTAGCGGAGTGTATA CTGG
hNR2F2-sub2	CAGAGCACACTCCGGGCTGGAGTGTTTTAAGATGTGTCTTCAA CAGGATGGCGATCGCATTAAATGATCCTAGAGCGCACGAAT GAGGG
hNR2F2-cherry-Q1	CGCCGCCCGCAGCCAGGGGAGCAGGAAGTCCGGACGCAGCC CCCATAGATATGGTGAGCAAGGGCGAGGAGGATAACATGGCC ATCATCAAGGAGTTC
hNR2F2-pA-Q2	GGGGCGCCGGGCGGGCCGGCCGGGCACGGGCGGCGCCTGCGA GGCCTGGCTATCATGACCATGATTACGCCAAGCTTGGGCTGC AGTTCTTTCCGCCTC
sgRNA 1	CAGCACGTGGCGCGACCCCC
sgRNA 2	GACGAGGTGCCCGGCTCACA

sgRNA 3	GCTGCCCTGTACCTCGTCCT
WT ss-DNA oligo	CATAGATATGGCAATGGTAGTCAGCACGTGGCGCGACCCCA GGACGAGGTGCCCGGCTCACAGGGCAGCCAGGCCTCGCAGGC GCCGCCGTGCCCGGCCCGCCGCCG

Sequences of screening primers for CRISPR/Cas9 targeting

Screening target	PCR Forward primer (5' – 3')	PCR Reverse primer (5' – 3')	Sequencing primer (5' – 3')
3' homology arm before BSD excision	CGGCAGTTGGGATTCG TGAATTG	CAGGATGTTAATCCACGG AGGGTC	-
3' homology arm after BSD excision	CCCACAACGAGGACTA CACCATC	CAGGATGTTAATCCACGG AGGGTC	-
5' homology arm	GCGGACCACTTTCATGC TGATTG	CTCCTCGCCCTTGCTCAC CAT	-
2nd allele screen	GCCAGACAAGCCATCG ACAAAAC	CGTAGTGCTTGCCGCTCG ACTTG	GCCAGACAAG CCATCGACAA AAC
9bp deletion in COUP-TFII	GCCAGACAAGCCATCG ACAAAAC	CTGTGAGCCGGGCACCTC GTC	GCCAGACAAG CCATCGACAA AAC

Off-target analysis

The websites CRISPR Design (<http://crispr.mit.edu>); CRISPR Finder (<http://www.sanger.ac.uk/htgt/wge/>); CRISPOR (<http://crispor.tefor.net>) and COD (<http://cas9.wicp.net>), which use either different algorithms or builds of the human genome, were used to identify potential off-target regions within annotated genes that the sgRNAs could anneal to. The top 4 or 5 candidates with 1 to 4 base mismatches were then evaluated for the presence of Cas9-induced mutations by PCR amplification of gDNA from both the targeted clones as well as the parental cell line. PCR amplicons were treated with Exonuclease I and Shrimp Alkaline Phosphatase (both NEB) and sequenced directly using primers matching sequences within the amplicon.

Sequences of sgRNA 1 off-target screening primers

Off-target	PCR Forward primer (5' – 3')	PCR Reverse primer (5' – 3')	Sequencing Primer (5' – 3')
GRIP2	GGAGTTGAGACAGAG TCGCAGAGC	CCAATCATCCTCCTCC TCCTCCTC	CTCAGAGGGCTGTGTAG ATGC
BRD2	ATGCTGAACTCGTATG GAGAGGC	CCACCATTGGTTAAGC ACTTGACT	CAGCCCCTCCCTTCCCG AAC
KL	GGACAAAGAGGTGGC TGAGAGAG	CAGTGAGGCACAAAA TGGATAGC	TACCTTTGAGAGCTTCG TTTATG
DNDH1	GTGCAGCCGGTCAGT GTAACAAC	GGCAGGTGAGGAATC GCAATG	TGCTGCAGGCGGTACTC ATAAG

Sequences of sgRNA 2 off-target screening primers

Off-target	PCR Forward primer (5' – 3')	PCR Reverse primer (5' – 3')	Sequencing Primer (5' – 3')
TMEM39B	TGACTGGCAGCTGGTATC ATTG	CCAGGCCTTTGGATTAT TCTACC	ATCTGTCCAAGT GATCACCTC
NMB	CAGGTCACCTTCATGGGCA AG	TAGACTGGGTGATGAGTC AGGG	TCTGCCTCAAGA GGGAAAAGCC
OSPBL3	CTGGCATGGGGACAGCA CAGTGA	TTGCCAATAGCTCTGGAC CGCC	AAAGTCCACCA AACCACAAAGG
CCDC167	AGGCAGAGCAGAACAGA CGGG	ACATTTACTCAGCAGACG GGAACAG	CCAGGAAGCCA TGCTTGAACAC
PCDH8	GCTGATCGTCATCATCGT GCTG	TACCTGAATGCACCCACC CTAC	ACGGCCGCAAG AAGGAGGTG

Sequences of sgRNA 3 (correction) off-target screening primers

Off-target	PCR Forward primer (5' – 3')	PCR Reverse primer (5' – 3')	Sequencing Primer (5' – 3')
BLK	TAACTCTGCCGGACTTGG TG	GTTTGGGGGTATCCCTCT GC	TAACTCTGCCGG ACTTGGTG
LACC1	GCTGCCCAATTTTCGTTGA GG	CATTCGGGACTTCTGTG GG	CATTCGGGACTT CCTGTCCG
ZNF44	TCGCAGGGAAACTTCGAC AA	TTGGACGAGGTACAAGG CAC	TCGCAGGGAAA CTTCGACAA
USH1C	GTCCCCAACTTTGGGTCA CA	GACCAGGAGATGACACT GCC	GTCCCCAACTTT GGGTCACA
BAIAP2	CCTTCCGCAGACCTGTCA GT	GCAGACTCCGTCCAGCTA CC	CCTTCCGCAGAC CTGTCACT

Cellular electrophysiology

Action potentials (APs) were recorded at $36 \pm 0.2^\circ\text{C}$ using the amphotericin-B perforated patch-clamp technique. The measurements were performed with an Axopatch 200B amplifier (Molecular Devices), and data acquisition and analysis were realized with custom software. Signals were low-pass-filtered with a cutoff of 5 kHz and digitized at 40 kHz. The potentials were corrected for the calculated liquid junction potential of 15 mV. Cell membrane capacitance (C_m) was determined with -5 mV voltage step from -40 mV by dividing the time constant of the decay of the capacitive transient by the series resistance. APs were recorded from spontaneously contracting hESC-derived CMs demonstrating regular and synchronous contractions at 2-10 s. Patch pipettes (borosilicate glass; resistance $\approx 2.5 \text{ M}\Omega$) contained (in mmol/L): 125 K-gluconate, 20 KCl, 5 NaCl, 0.44 amphotericin-B, 10 HEPES; pH 7.2 (KOH). Bath solution was composed of (in mmol/L): 140 NaCl, 5.4 KCl, 1.8 CaCl_2 , 1.0 MgCl_2 , 5.5 glucose, 5.0 HEPES; pH 7.4 (NaOH). hPSC-derived CMs typically lack the inward rectifier K^+ current, I_{K1} , that limits

the functional availability of the Na⁺ current (I_{Na}) and transient outward K⁺ current (I_{To}). To overcome this limitation, we injected an in silico I_{K1} with kinetics of Kir2.1 channels through dynamic clamp, as we previously described in detail. An amount of 2 pA/pF peak outward current was applied, resulting in quiescent hPSC-CMs with a maximal membrane depolarization (MDP) of -80 mV or more negative. APs were elicited at 0.5 to 4 Hz by 3 ms, ~1.2 \times threshold current pulses through the patch pipette. AP parameters that were characterized were MDP, maximum AP amplitude (APA_{max}), AP duration at 20, 50 and 90% of repolarization (APD₂₀, APD₅₀, and APD₉₀ respectively), maximal upstroke velocity (V_{max}) and plateau amplitude (APA_{plat}) measured 20 ms after the AP upstroke). Averages were taken from 10 consecutive AP.

Transcriptional analysis and qPCR

Total RNA was isolated with the NucleoSpin RNA isolation Kit (Macherey-Nagel) according to manufacturer's protocol. For qPCR, cDNA was synthesized with iScript cDNA Synthesis Kit (BIO-RAD). Data was normalized to hARP as housekeeping gene. qPCR was carried out in triplicate reactions for each target using SybrGreen master mix (Applied Biosystems) and the CFX384 Real-time PCR detection system with a 3-Step protocol (30 s at 95°C, followed by 40 cycles of 95°C for 5 s and 60°C for 30 s). Primer sequences are provided in Suppl. table 5. Data was analyzed with Bio-Rad CFX Manager software and normalized to hARP as housekeeping gene. The number of independent biological replicates for each experiment are noted in figure legends.

Sequences of qPCR primers

	Forward (5' – 3')	Reverse (5' – 3')
<i>ACTA2</i>	GCACCCCTGAACCCCAAGGC	AGCACGATGCCAGTTGTGCGT
<i>COUP-TFII</i>	AAGCCATCGTGCTGTTCAC	GCTCCTCACGTACTCCTCCA
<i>COUP-TF I</i>	TTTTCCTGCAAGCTTTCCAC	CCGAGTACAGCTGCCTCAA
<i>TNNT2</i>	AGCATCTATAACTTGGAGGCAGA G	TGGAGACTTTCTGGTTATCGTT G
<i>GJA5</i>	TCTTTCCCTAACCCGATCC	TGTCCCTGGCCTTGAATATC
<i>hARP</i>	CACCATTGAAATCCTGAGTGATGT	TGACCAGCCCAAAGGAGAAG
<i>HEY1</i>	AGTTGCGCGTTATCTGAGC	TGTTGAGATGCGAAACCAG
<i>HEY2</i>	GATTCAGCCCTCCGAATG	TGGCAGAGAGGGACAAGAG
<i>IRX4</i>	TTCCGTTCTGAAGCGTGGTC	TGAAGCAGGCAATTATTGGTGT
<i>KCNA5</i>	CGAGGATGAGGGCTTCATTA	CTGAACTCAGGCAGGGTCTC
<i>KCNJ5</i>	CACCCTGGTGGACCTCAAGTGGC GC	AGCTCCGGGCTTGGCAGGTCAT GC
<i>KCNJ3</i>	TGTCGTCATCCTAGAAGGCA	AAAAACGATGACCCCAAAGA
<i>MYL2</i>	GATGTTCCGCCCTTCCCCC	GCAGCGAGCCCCCTCCTAGT
<i>PECAMI</i>	GCAAAAATGGGAAGAACCTGA	CACTCCTTCCACCAACACCT
<i>PITX2</i>	GTGTGGACCAACCTTACGGA	AGCCATTCTTGCATAGCTCG
<i>NR2F2-001</i>	GCAAGCACTACGGCCAGTT	CTGCGCTTGAAGAAGCTCTT
<i>NR2F2-002</i>	AGCAGGGAAATATATCCGGACAG G	CCCTCTGCACCGCAAAA

NR2F2-201	GTCCTGGGTACGTTTGGCTA	CAGGTACGAGTGGCAGTTGA
NR2F2-003	GCAGTAAAGAAGAAAGATGCCCT C	AGCAGGGAAATATATCCGGAC AGG

Flow cytometry

hESCs were stained for TRA-1-60 with human Anti-TRA-1-60-PE (1:11) (Clone REA157; Miltenyi Biotech) at RT for 10 min and analyzed by flow cytometry. For flow cytometric analysis of endothelial and SMC markers, RA-treated cultures were stained for CD31-APC (Clone WM59; ebioscience), CD144-PE-Cy7 (Clone 16BI; ebioscience) and CD90-PE-Vio770 (Clone DG3; Miltenyi Biotech) at 4°C for 20 min and were analyzed with a BD ARIA III flow cytometer. To eliminate cell debris or aggregated cells, events with very low or high side and forward scatter were excluded. Subsequent data analysis was performed with MACSQuantify™ or FlowLogic Software and results are expressed as mean ± SEM of percentage of cells.

Immunostaining and confocal imaging

D14 differentiations were dissociated and re-plated on Matrigel-coated glass coverslips and fixed in 2% paraformaldehyde, followed by permeabilization with 0.1% Triton X 100 (Sigma Aldrich) in PBS. Blocking was performed with 4% swine serum (Dako) in PBS and cells were incubated overnight at 4°C with primary antibodies rabbit anti-troponin I (clone H170, Santa Cruz; 1:1500), rat anti-mCherry (M11217 GIBCO, Thermo Fisher Scientific; 1:250), mouse anti-SMA (A2547 Sigma-Aldrich; 1:250), mouse anti-PECAM (M082301, Dako; 1:100) and rabbit anti-AFP (2011200530, Quartett, 1:30). Detection of primary antibodies was achieved by incubation with corresponding secondary antibodies conjugated to Alexa Fluor 647 (anti-rabbit (A-31573) or anti-mouse (A-31571); Invitrogen); anti-rat Alexa-555 (A-21434; Invitrogen) and anti-rabbit-Cy3 (711-165-152, Jackson Immuno Research), all 1:250 for 1h at RT. Nuclei were stained with 4', 6-Diamidino-2-Phenylindole (DAPI) (Invitrogen) at RT for 5 min and coverslips were embedded with Prolong gold (P36930; Invitrogen). Confocal images were captured with an inverted Leica TCS SP5 or SP8WLL microscope (Leica Microsystems). Optical z-stacks were acquired with a 40x, 63x or 100x oil immersion objective and image acquisition was performed with LAS AF software (Leica Microsystems).

Supplemental videos

Supplemental video 1: Contracting RA-treated M⁺ Spin-EB at day 14 of differentiation.

Supplemental video 2: Contracting RA-treated and CT Spin-EB from COUP-red hESCs at day 14 of differentiation merged with GFP and mCherry.

Supplemental video 3: Contracting R and CT Spin-EB from WT NKX-GFP hESCs at day 14 of differentiation merged with GFP and mCherry.

Supplemental video 4: Contracting RA and CT Spin-EB from COUP-KO 1 hESCs at day 14 of differentiation merged with GFP and mCherry.

Supplemental references

1. Kranz A, Fu J, Duerschke K, Weidlich S, Naumann R, Francis Stewart A, Anastassiadis K. An improved flp deleter mouse in C57Bl/6 based on flpo recombinase. *Genesis*. 2010;48:512–520.